

Flexible Local Approximation Models for Wave Scattering in Photonic Crystal Devices

H. Pinheiro¹, J. P. Webb¹, and I. Tsukerman²

¹Department of Electrical and Computer Engineering, McGill University, Montreal, QC, H3A 2A7, Canada

²University of Akron, Akron, OH 44325-3904 USA

The dominant mode of a photonic crystal (PC) waveguide is computed by an eigenvalue formulation of the flexible local approximation method (FLAME). The computed mode is then incorporated into a new excitation-absorption boundary condition for use in predicting scattering in multiport PC devices. Reflection and transmission coefficients of several devices are calculated by the new method; agreement with previously published values is excellent.

Index Terms—Dielectric waveguides, electromagnetic scattering, finite difference methods, optical planar waveguides.

I. INTRODUCTION

IN the recently developed flexible local approximation method (FLAME), accurate local approximations of the solution are incorporated directly into a difference scheme, which in many cases significantly increases the numerical accuracy. The method is ideally suited to the solution of problems consisting of large numbers of similar structures, such as the dielectric rods (or holes) in a photonic crystal (PC) device [1]. Indeed, FLAME has already been used to solve the wave equation inside a PC device [2]. However, to predict reflection and transmission properties two steps are needed: first, to compute the dominant modes of the PC waveguides attached to the ports [3] and second, to solve for the field in the device with the modes as the excitation, being careful to absorb the outgoing radiation. FLAME methods for these steps are developed in this paper.

II. TREFFTZ FLAME FOR SCATTERING

PC devices are commonly analyzed in 2-D, assuming no field variation with z . With a time-harmonic transverse magnetic (TM) excitation, the governing equation is

$$\nabla^2 \phi + n^2(\omega/c)^2 \phi = 0 \text{ in } \Omega \quad (1)$$

where ϕ is the z component of the complex electric field; n is the refractive index, a function of x and y ; ω and c are, respectively, the angular frequency and the vacuum velocity of light; and Ω is the computational domain in the $x - y$ plane. In the Trefftz-FLAME method, the starting point is a regular grid of nodes over Ω . One equation is generated for each node, using a 3×3 computational molecule centered on that node. The equation is constructed using a set of eight basis functions, each of which satisfies (1) exactly within the molecule. When the molecule contains no part of a rod, the basis functions are chosen

to be eight plane waves, propagating in equally spaced directions. When any part of a rod is present in the molecule, the basis functions are eight cylindrical wave functions centered on the rod axis. Details are in [2].

There are two kinds of boundary conditions to consider (see, for example, the inset geometry in Fig. 3). Some boundary lines are intersected by the PC waveguides that carry energy into or out of the device. These are the ports of the device and how they are handled is shown in Section III. The remaining boundary lines represent a truncation of a theoretically infinite array of rods. For each node on this boundary, a perfectly matched layer (PML)-FLAME equation is added to the system. This is an approximate absorbing condition, discussed in [2].

III. TREFFTZ FLAME FOR THE WAVEGUIDE MODE

In order to apply a suitable boundary condition to the ports, it is first necessary to compute the field of the dominant mode of the waveguide passing through that port, together with its phase constant β . Fig. 1 shows a port with a short length of waveguide connected to it, and a FLAME grid superimposed. The shaded region is used in the modal analysis. The governing equation remains (1), with the value of ω as required for the subsequent scattering analysis. On the lines Γ_1 and Γ_2 , it is necessary to apply the Bloch-Floquet boundary condition $\phi(a, y) = \mu \phi(0, y)$, where $\mu = e^{-j\beta a}$. This is done as follows. An extra row of nodes is placed outside the port, as shown in Fig. 1. For nodes $i = 1, \dots, n - 1, j = 1, \dots, m$, the same Trefftz-FLAME equations are constructed as described in Section II—including the use of PML-FLAME for the nodes on the left and right boundaries ($j = 1$ and $j = m$).

Then, the following $2m$ equations are added, to enforce the periodic condition:

$$\begin{aligned} \phi_{nj} &= \mu \phi_{1j}, & j &= 1, \dots, m \\ \phi_{n-1,j} &= \mu \phi_{0j}, & j &= 1, \dots, m. \end{aligned} \quad (2)$$

The result is $(n + 1)m$ equations in the same number of nodal unknowns. The parameter μ is also unknown, but becomes the

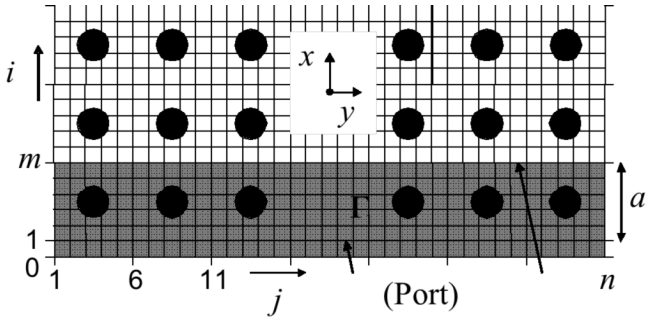


Fig. 1. Port and short length of a typical PC waveguide. The waveguide axis is in the x direction. Energy is largely confined to the “defect” in the middle. The shaded area is used for finding the modes.

eigenvalue. The set of equations can be arranged into the following form:

$$[A]\{\phi\} = \mu[B]\{\phi\}. \quad (3)$$

Matrices $[A]$ and $[B]$ are sparse, but not Hermitian; since they are relatively small, the MATLAB dense-matrix QZ algorithm can be used for the eigenproblem. This gives ϕ^+ , the dominant mode propagating in the $+x$ direction along the periodic waveguide, along with its associated value of μ , from which β is obtained. It also gives ϕ^- , the dominant mode propagating in the $-x$ direction. By symmetry, ϕ^- has phase constant $-\beta$, and provided ϕ^+ and ϕ^- are normalized in the same way

$$\begin{aligned} \phi_{1j}^- &= \phi_{nj}^+, & j &= 1, \dots, m \\ \phi_{nj}^- &= \phi_{1j}^+, & j &= 1, \dots, m. \end{aligned} \quad (4)$$

IV. PORT BOUNDARY CONDITION

Let ϕ^+ and ϕ^- correspond to waves incident on a port and leaving a port, respectively. Then, if we assume that only these fields are present, the total field on the port is given by

$$\phi = V^+\phi^+ + V^-\phi^- \quad (5)$$

where V^+ and V^- are two complex coefficients defining the amounts of the incident and outgoing waves, respectively. We specify V^+ for each port, but do not know V^- ; we need a boundary condition that sets up the incident wave and absorbs the outgoing wave. From (5) and (2)

$$\begin{aligned} \phi_{1j} &= V^+\phi_{1j}^+ + V^-\phi_{1j}^-, & j &= 1, \dots, m \\ \phi_{nj} &= V^+\phi_{nj}^+ + V^-\phi_{nj}^- \\ &= V^+\phi_{1j}^+e^{-j\beta a} + V^-\phi_{1j}^-e^{j\beta a}, & j &= 1, \dots, m. \end{aligned} \quad (6)$$

Eliminating $V^-\phi_{1j}^-$ from these equations gives

$$e^{j\beta a}\phi_{1j} - \phi_{nj} = V^+\phi_{1j}^+2j \sin \beta a, \quad j = 1, \dots, m. \quad (7)$$

This set of equations constitutes the boundary condition needed for the port. Note that, for an unexcited port, V^+ is set to zero.

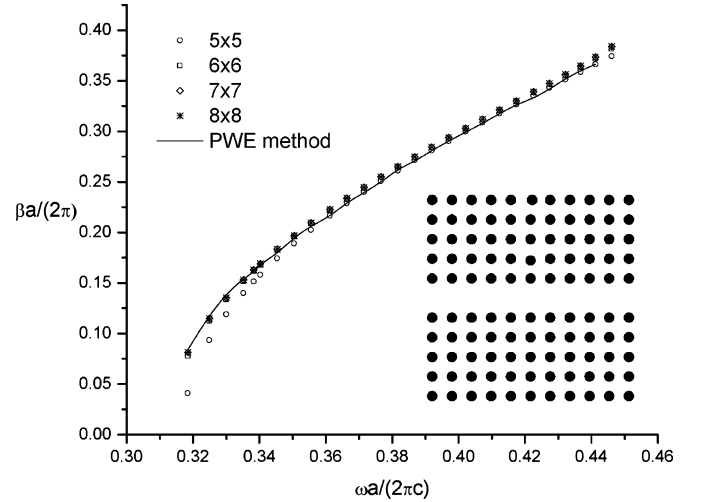


Fig. 2. Dispersion curves for a PC waveguide. The $a \times a$ lattice cell is modeled with 5×5 (circles), 6×6 (squares), 7×7 (triangles), and 8×8 (stars) grid points. The solid line is from [1], obtained by the PWE method.

After solution, the value of V^- can be extracted using (6), (4), and (2)

$$\begin{aligned} \phi_{1j} &= V^+\phi_{1j}^+ + V^-\phi_{1j}^- \\ &= V^+\phi_{1j}^+ + V^-\phi_{nj}^+ \\ &= V^+\phi_{1j}^+ + V^-\phi_{1j}^+e^{-j\beta a}, \quad j = 1, \dots, m. \end{aligned} \quad (8)$$

Rearranging

$$V^- = (\phi_{1j} - V^+\phi_{1j}^+) / (\phi_{1j}^+e^{-j\beta a}), \quad j = 1, \dots, m. \quad (9)$$

In theory, each node j should give the same value of V^- ; in practice, the right-hand side of (9) is averaged over all the nodes on the port.

The power reflection coefficients given in Section V are the values $|V^-/V^+|^2$. The same expression is used for the transmission coefficients, but in this case V^+ is for one port and V^- for another (with the same waveguide dimensions at each). The coefficients are plotted directly as ratios, rather than in decibels, since this is customary in the PC literature.

V. RESULTS

For all simulations, the waveguides are made of a square lattice of dielectric rods (refractive index 3.4) in air with radius $r = 0.18a$, where a is the lattice constant.

In order to treat PC waveguides, first, the eigenmodes of the periodic waveguide are calculated following the method described in Section IV. Fig. 2 shows the normalized propagation constant $\beta a / 2\pi$ of the TM mode guided along a line defect, as a function of normalized frequency $\omega a / (2\pi c)$. The results show that we can model the $a \times a$ lattice cell with 6×6 points and obtain results that agree well with those of the plane wave expansion (PWE) method [1].

Next, we apply FLAME to a 90° bend. The fundamental TM mode is incident at port 1. Fig. 3 shows that the results obtained using 8×8 nodes per lattice cell, giving 7744 degrees of freedom (DOFs). These results agree well with those

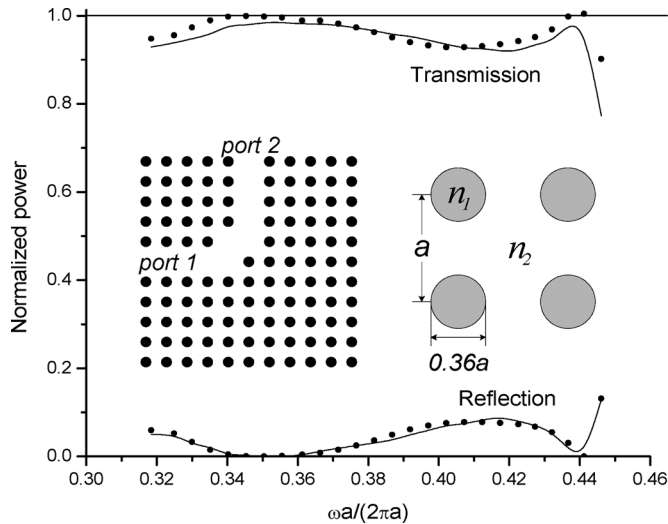


Fig. 3. Transmission and reflection coefficients of a 90° waveguide bend. Circles represent FLAME and solid lines represent FETD-BPM [4] results.

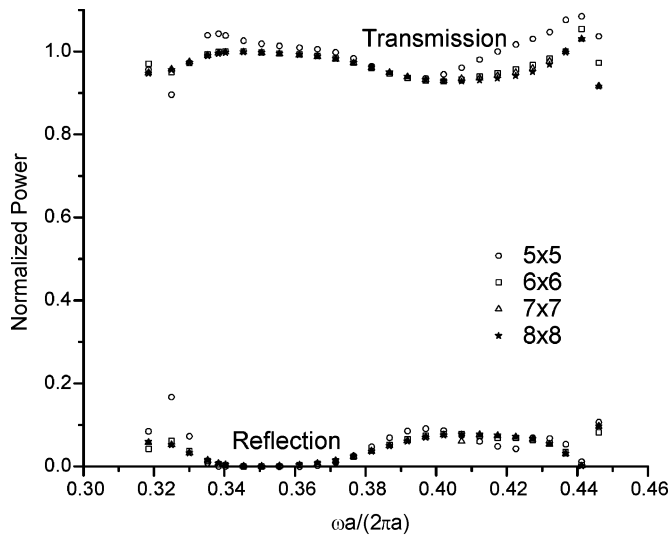


Fig. 4. Convergence of the results for the PC bend. The lattice cell is modeled with 5×5 (circles), 6×6 (squares), 7×7 (triangles), and 8×8 (stars) grid points.

calculated by the finite-element time-domain beam propagation method (FETD-BPM) using 158 607 DOFs [4]. Note that, at one frequency, the FLAME transmission coefficient is very slightly greater than 1 (actually 1.016). This is the result of the discretization error; nothing in FLAME explicitly imposes power conservation.

Fig. 4 shows, for the same device, the transmission and reflection coefficients as a function of a normalized frequency $\omega a/(2\pi c)$ when the lattice cell is modeled with 5×5 , 6×6 , 7×7 , and 8×8 nodes. It can be seen that the convergence is fast and that there is no significant difference in the results when 6×6 , 7×7 , or 8×8 grid points are used.

The FLAME results for a Y -branch are shown in Fig. 5. Port 1 is excited and from the field solution the reflection coefficient at port 1 and the transmission coefficients to ports 2 and 3 were computed. The results obtained are in very good agreement with those of FETD-BPM [4].

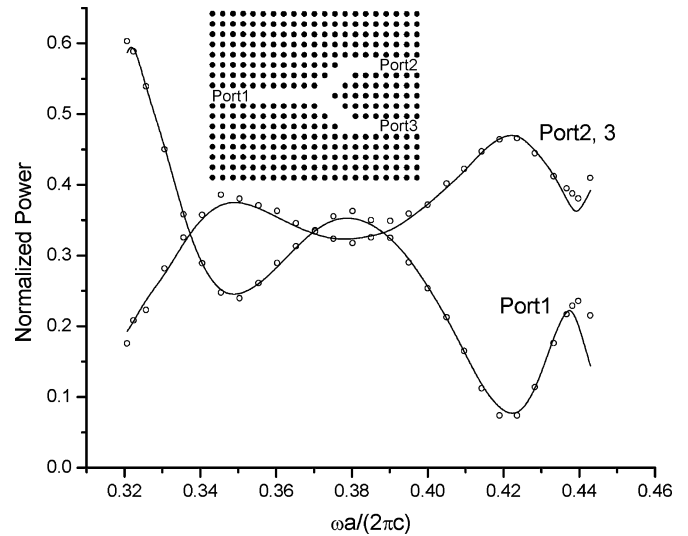


Fig. 5. Transmission and reflection coefficients of a Y -branch waveguide. Circles represent FLAME and solid lines represent FETD-BPM [4] results.

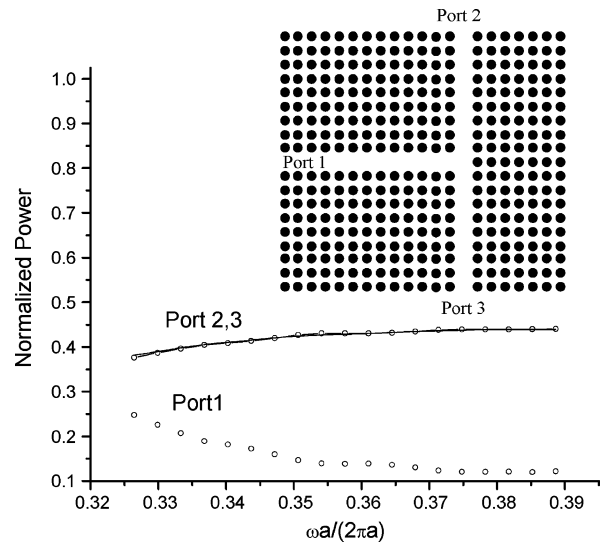


Fig. 6. Transmission and reflection coefficients of a T -branch waveguide. Circles represent FLAME and the solid line represents FDTD results [5].

Next, we apply FLAME to a T -branch (Fig. 6). Again, port 1 is excited. FLAME results agree well with those of the finite-difference time-domain (FDTD) method [5], also plotted. In the FDTD simulation, the lattice cell was modeled with 15×15 grid points, whereas in the FLAME simulation only 8×8 grid points were used.

An example of a four-port device is the directional coupler shown in Fig. 7. Power injected at port 1 is coupled to three other ports to varying degrees. Once again, there is good agreement with FETD-BPM results [4].

Finally, we consider a microcavity coupled to straight waveguides (Fig. 8). At the frequency of a cavity resonance, there is a strong transmission from port 1 to port 2, which FLAME is able to capture.

Some idea of the relative efficiency of the FLAME approach to PC device analysis is given in Table I, which gives the number of rods in the computational domain and the number of

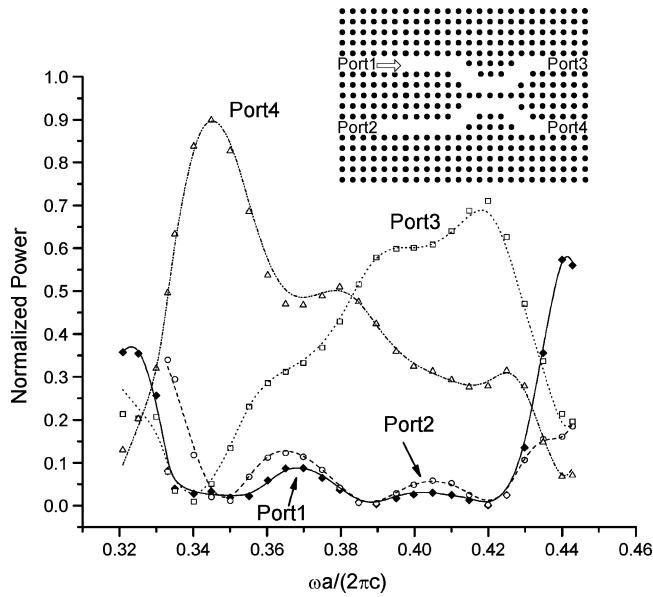


Fig. 7. Transmission and reflection coefficients of a directional coupler. Circles, squares, triangles, and solid diamonds represent FLAME results and the lines represent FETD-BPM results [4].

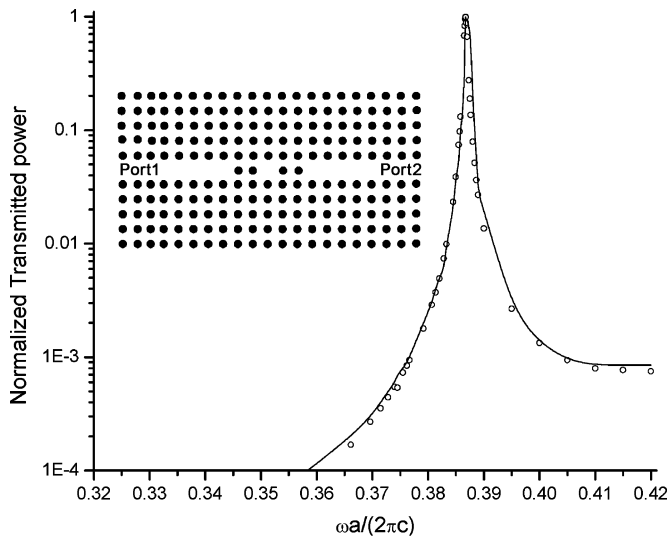


Fig. 8. Transmission coefficient of a microcavity. Circles represent FLAME results and the solid line represents FETD-BPM results [4].

DOFs for FLAME and for competing methods. In each case, the computational domain (number of rods) needed by FLAME is significantly smaller than for FETD-BPM and FDTD. This, together with the coarser gridding needed per lattice cell, gives a much lower number of DOFs. The FLAME matrices for the scattering problem are not only modest in size, but also very sparse. Solution times for the matrix problem using a direct, sparse solver were less than 2 s per frequency point (on a Pentium 4, 3-GHz processor), for all of the problems presented.

VI. CONCLUSION

The FLAME has been presented for computing the propagating mode of a PC waveguide. It has been shown how the

TABLE I
RELATIVE EFFICIENCY OF FLAME

| Structure | Method | Ref. | Rods | DOFs |
|-------------|----------|------|-----------|-----------|
| Bend | FLAME | | 11 × 11 | 7,744 |
| | FETD-BPM | [4] | 638 | 158,607 |
| Y-Branch | FDTD | [6] | 101 × 121 | |
| | FLAME | | 21 × 17 | 22,848 |
| Coupler | FETD-BPM | [4] | 65 × 17 | |
| | FLAME | | 24 × 17 | 26,112 |
| T-Branch | FETD-BPM | | 65 × 17 | |
| | FLAME | | 21 × 19 | 25,536 |
| Microcavity | FDTD | [5] | 141 × 181 | 5,742,225 |
| | FLAME | | 19 × 11 | 13,376 |
| | FETD-BPM | | 65 × 11 | |

computed mode can be used to provide port boundary conditions for a PC multiport device, and to extract reflection and scattering coefficients. Computational efficiency is the result of FLAME's ability to model the circular rods with a relatively coarse grid, and is also due to the small size of the computational domain needed for this frequency-domain, mode-driven analysis. Although only square lattices have been tried so far, the method could equally be applied to other lattice types, e.g., triangular. In addition, the computational advantages of FLAME are expected to be even more pronounced when it is applied to the 3-D geometries.

ACKNOWLEDGMENT

This work was supported by the Natural Sciences and Research Council of Canada.

REFERENCES

- [1] J. D. Joannopoulos, R. D. Meade, and J. N. Winn, *Photonic Crystals*. Princeton, NJ: Princeton Univ. Press, 1995.
- [2] I. Tsukerman, "Electromagnetic applications of a new finite-difference calculus," *IEEE Trans. Magn.*, vol. 41, no. 7, pp. 2206–2225, Jul. 2005.
- [3] Y. Tsuji and M. Koshiba, "Finite element method using port truncation by perfectly matched layer boundary conditions for optical waveguide discontinuity problems," *J. Lightw. Technol.*, vol. 20, no. 3, pp. 463–468, Mar. 2002.
- [4] M. Koshiba, Y. Tsuji, and M. Hikari, "Time-domain beam propagation method and its application to photonic crystal circuits," *J. Lightw. Technol.*, vol. 18, no. 1, pp. 102–110, Jan. 2000.
- [5] S. Fan, S. G. Johnson, and J. D. Joannopoulos, "Waveguide branches in photonic crystals," *J. Opt. Soc. Amer. B, Opt. Phys.*, vol. 18, no. 2, Feb. 2001.
- [6] A. Mekis, J. C. Chen, I. Kurland, S. Fan, R. Villeneuve, and J. D. Joannopoulos, "High transmission through sharp bends in photonic crystal waveguides," *Phys. Rev. Lett.*, vol. 114, pp. 185–200, Oct. 1994.